Validity of the Harris criterion for two-dimensional quantum spin systems with quenched disorder

Jhao-Hong Peng ⬥, L.-W. Huang, D.-R. Tan ⬥, and F.-J. Jiang ⬥[*]

Department of Physics, National Taiwan Normal University, 88, Section 4, Ting-Chou Road, Taipei 116, Taiwan

Inspired by the recent results regarding whether the Harris criterion is valid for quantum spin systems, we have simulated a two-dimensional spin-1/2 Heisenberg model on the square lattice with a specific kind of quenched disorder using the quantum Monte Carlo calculations. In particular, the considered quenched disorder has a tunable parameter $0 \leqslant p \leqslant 1$ which can be considered as a measure of randomness. Interestingly, when the magnitude of p increases from 0 to 0.95, at the associated quantum phase transitions the numerical value of the correlation length exponent ν grows from a number compatible with the $O(3)$ result 0.7112(5) to a number slightly greater than 1. In other words, by varying p, ν can reach an outcome between 0.7112(5) and 1 (or greater). Furthermore, among the studied values of p, all the associated ν violate the Harris criterion except the ones corresponding to $p \geqslant 0.9$. Considering the form of the employed disorder here, the above described scenario should remain true for other randomness if it is based on an idea similar to the one used in this study. This is indeed the case according to our preliminary results stemming from investigating another disorder distribution.

I. INTRODUCTION

Studying the effects resulting from disorder has always been one of the major topics in both theoretical and experimental physics [1–15]. This is because the presence of disorder such as impurities may lead to extraordinary properties and phases of materials. In particular, the appearance of these exotic characteristics are due to the mutual influence between the quantum fluctuations and disorder. Understanding the relevance of disorder at quantum phase transitions also continues to attract a lot of attention. This is especially true considering the recent development regarding under what conditions the celebrated Harris criterion will be valid [16–27]. In other words, it is not clear at all what specific features of a disorder distribution lead to a new universality class at the associated quantum phase transition.

For a phase transition, there are three possible scenarios when disorder is present. Here we will focus on those related to the Harris criterion. The Harris criterion was originally derived for classical systems and its statement is as follows. For a D-dimensional classical system with disorder, the correlation length exponent ν must satisfy the inequality $\nu \geqslant 2/D$. If the ν of a clean model does not fulfill this inequality, then when disorder is introduced (into the clean model), a new universality class should be obtained so that the described inequality is realized, assuming the phase transition remains well defined. Later the criterion was generalized to more generic situations including certain quantum systems. We would like to emphasize the fact that for a d-dimensional quantum system with quenched disorder, since the disorder is employed in the spatial dimension, the dimensionality D appearing in the inequality is d, not $d + 1$, despite that

the quantum system can be mapped to a $d + 1$-dimensional classical system.

While the validity of Harris criterion is beyond doubt for classical models, the case of quantum spin systems is much more complicated. Particularly, for the dimerization circumstances, at the moment only the outcome related to the two-dimensional (2D) spin-1/2 Heisenberg model on a bilayer square lattice with site (dimer) dilution satisfies the Harris criterion [19–23]. Other kinds of quenched disorder, including the configurational disorder considered in Ref. [10] as well as the one introduced in Ref. [15], the resulting calculations always indicate the Harris criterion is violated. Furthermore, the obtained values of the correlation length exponent ν remain the same as that of their clean counterparts. To summarize, whether the celebrated Harris criterion is valid for quantum spin systems is more involved than anticipated.

Inspired by such an indecisive answer regarding the applicability of Harris criterion for quantum spin systems, in this study we have carried out large scale quantum Monte Carlo (QMC) calculations for a two-dimensional spin-1/2 Heisenberg model on the square lattice, starting from the clean herringbone model and then introducing a specific kind of quenched disorder into the clean system. In particular, the employed randomness distribution has a tunable parameter p (which can take values from 0 to 1 and can be considered as a measure of randomness) so that one can investigate the impact of this parameter on the effectiveness of Harris criterion for the studied model.

Remarkably, our QMC data indicate that as the magnitude of p increases gradually from 0 to 0.95, the numerical value of ν grows from its $O(3)$ value 0.7112(5) [28–35] to a result slightly greater than 1. In other words, by varying p, the corresponding ν for the disordered systems studied in this investigation can reach outcomes that lie between 0.7112(5) and 1. Moreover, the ν resulting from the considered values
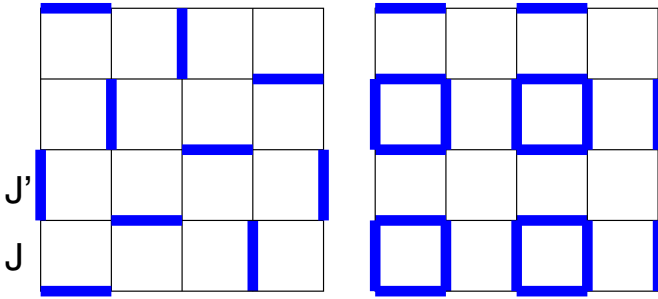
---

*fjjiang@ntnu.edu.tw

FIG. 1. The 2D herringbone (left) and plaquette (right) spin-1/2 Heisenberg models on the square lattice investigated here. The antiferromagnetic coupling strengths for the thick and thin bonds are J' and J, respectively. Quenched disorder is introduced into the systems by considering certain kinds of distribution in antiferromagnetic strengths for the thick bonds; see the main text for the details.

of p all violate the Harris criterion except the ones related to $p \geqslant 0.9$. This result implies that there exists a p_c so that the ν, which corresponds to p greater (smaller) than p_c, will fulfill (violate) the Harris criterion.

Our preliminary study of another disorder distribution following the similar idea as that introduced above leads to the same conclusion, particularly ν can take a value between 0.7112(5) and 1. The outcomes demonstrated here indicate that a better understanding of the Harris criterion from a theoretical point of view is on request.

The rest of the paper is organized as follows. After the Introduction, the model, the employed disorder distribution, and the observables are described. Then the numerical outcomes are demonstrated. In particular, convincing evidence which supports the exotic scenario introduced above is provided. Finally, a section is devoted to conclude the works presented here. The Appendix contains more data as well as the analysis procedures employed in this study.

II. MICROSCOPIC MODELS AND OBSERVABLES

The left panel of Fig. 1 demonstrates the herringbone model on the square lattice. In addition, the corresponding Hamiltonian is given by

$$H = \sum_{\langle ij \rangle} J \vec{S}_i \cdot \vec{S}_j + \sum_{\langle i'j' \rangle} J' \vec{S}_{i'} \cdot \vec{S}_{j'}, \qquad (1)$$

where in Eq. (1) J (which is set to 1) and J' are the antiferromagnetic couplings (bonds) connecting nearest-neighbor spins $\langle ij \rangle$ and $\langle i'j' \rangle$ located at sites of the considered underlying square lattice, respectively, and $\vec{S}_i$ is the spin-1/2 operator at site i. The quenched disorder introduced into the system is based on the one employed in Ref. [15]. Specifically, for every bold bond in the left panel of Fig. 1, its antiferromagnetic strength J' takes the value of $1 + (g-1)(1 + p)$ or $1 + (g-1)(1 - p)$ with equal probability. Here $g > 1$ and $0 \leqslant p \leqslant 1$. As pointed out in Ref. [15], the average and difference of J' for these two types of bold bonds are given by g and $2p(g-1)$, respectively. Moreover, p can be considered as a measure of disorder of the studied system. In our study, several values of p are chosen and for each of them, the corresponding phase transition is induced by tuning g.

To carry out the proposed investigation, particularly to examine the validity of Harris criterion for the considered disordered model, the observables first Binder ratio Q_1 and second Binder ratio Q_2 [36], which are defined by

$$Q_1 = \frac{\langle |m_s^z| \rangle^2}{\langle (m_s^z)^2 \rangle} \qquad (2)$$

and

$$Q_2 = \frac{\langle (m_s^z)^2 \rangle^2}{\langle (m_s^z)^4 \rangle}, \qquad (3)$$

respectively, are measured in our calculations. The staggered magnetization density m_s^z on a square lattice with linear box size L appearing above is given by $m_s^z = \frac{1}{L^2} \sum_i (-1)^{i_1+i_2} S_i^z$ with S_i^z being the third component of the spin-1/2 operator $\vec{S}_i$ at site i.

Q_1 and Q_2 are chosen as the relevant physical quantities for our investigation because their expected finite-size scaling formulas [31],

$$Q_i = (1 + b_i L^{-\omega}) f_i (t L^{1/\nu}), \ i \in \{1, 2\},$$
$$t = \frac{g - g_c}{g_c}, \qquad (4)$$

do not contain the dynamic critical exponent z. Such a strategy, namely using Q_1 and Q_2 in our study, dramatically eliminates the computational complexity.

III. NUMERICAL RESULTS

For each of the studied p, to investigate the g dependence of the correlation length exponent ν associated with it, we have carried out a large scale QMC simulation using the stochastic series expansion (SSE) algorithm with very efficient operator-loop update [37,38]. Furthermore, to obtain ground-state properties in an efficient manner, the β-doubling scheme described in Ref. [3] is used in our simulations. Several hundred disordered configurations, each with its own random seed, are generated for every considered set of parameters. It is also important to notice that potentially there are two kinds of uncertainties for the used observables, namely the one from Monte Carlo (MC) simulations and the one from disorder averaging. We have carried out many trial simulations and have reached the conclusion that with the MC sweeps employed in this study, the resulting errors of the considered quantities are indeed dominated by the disordered sample-to-sample fluctuation.

The method used for the determination of ν (and g_c as well) is the Bayesian analysis which is a rigorous mathematical approach. It is demonstrated in Refs. [39,40] that the critical exponents calculated using the Bayesian analysis agree quantitatively with those determined by the conventional fits using the idea of finite-size scaling. Here we follow the methods outlined in Ref. [41]. Moreover, We have carried out many trial computations and have arrived at the same conclusion as those in Refs. [39,40], namely the results obtained from the Bayesian analysis and the conventional finite-size scaling fits are consistent with each other quantitatively. Such comparisons between the results obtained by two different methods
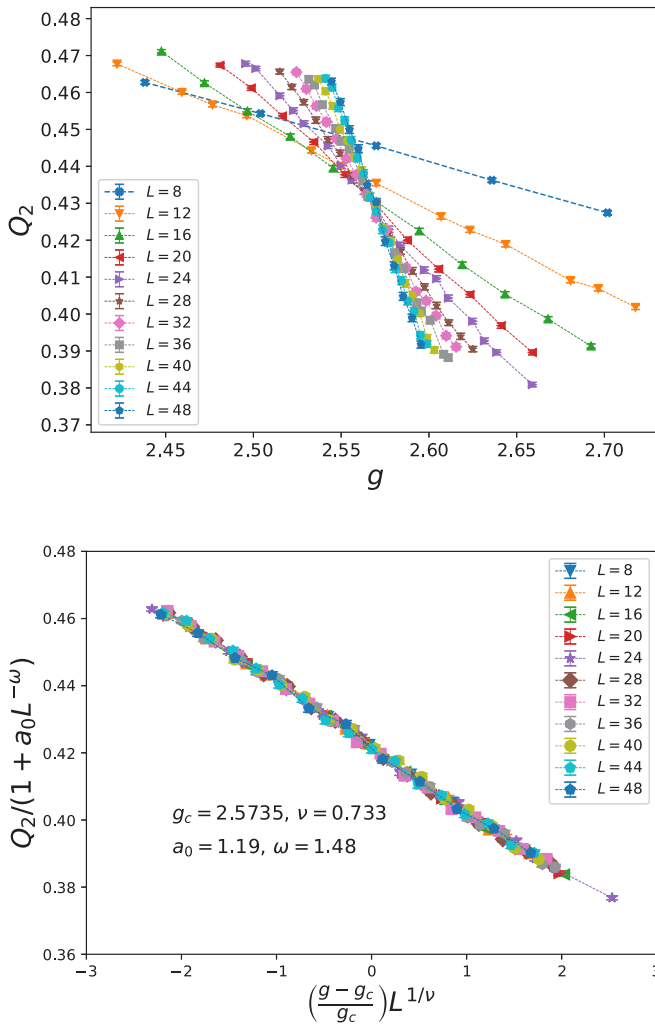
FIG. 2. Q_2 (top panel) of $p = 0.3$ and the corresponding data collapse (bottom panel) of the considered herringbone model studied here. Dashed lines are added to guide the eye. The g_c, ν, a_0, and ω shown in the bottom figure, which are used to produce the demonstrated results, are obtained from one of the many associated analyses

for $p = 0.5$ and $p = 0.9$ are listed in Tables II and III of the Appendix.

The model considered for the Bayesian analysis is the expected finite-size scaling equations for Q_1 and Q_2 at a second-order phase transition. Specifically, the explicit expression of the model for the Bayesian analysis is given by

$$(1 + a_0 L^{-\omega})(a_1 + a_2 t L^{1/\nu} + a_3 (t L^{1/\nu})^2 + \cdots). \qquad (5)$$

Here a_i for $i = 0, 1, 2, \ldots$ are some constants and $t = \frac{g - g_c}{g_c}$. Moreover, this *Ansatz* with up to third, fourth, and fifth order in $t L^{1/\nu}$ are employed in the calculations of estimating the desired physical quantities ν and g_c with the data of Q_1 and Q_2. Some constraints, such as the range of g considered and the values of ω obtained, are taken in account in the procedure of analysis as well. Q_2 of $p = 0.3$ as well Q_1 of $p = 0.9$ and the corresponding data collapse are shown in Figs. 2 and 3.

Table I summarizes the final quoted values of ν and g_c for all the considered p. This table is based on the results of
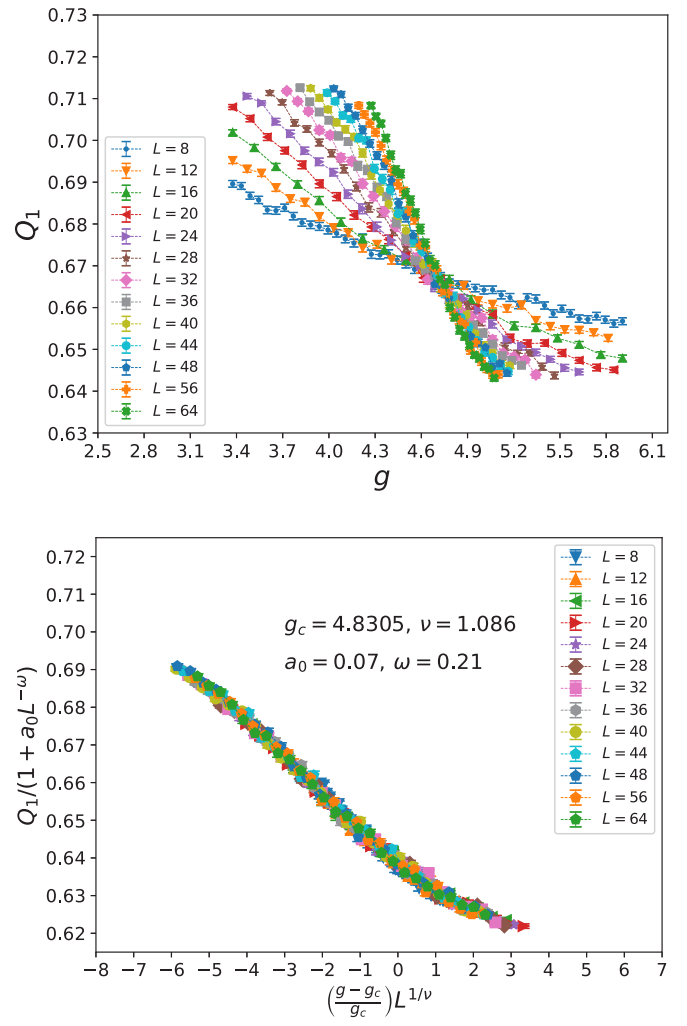
FIG. 3. Q_1 (top) of $p = 0.9$ and the corresponding data collapse (bottom) for the considered disordered herringbone model studied here. Dashed lines are added to guide the eye. The g_c, ν, a_0, and ω shown in the bottom figure, which are used to produce the demonstrated result, are obtained from one of the many associated analyses

each individual p obtained from the Bayesian analysis. The bootstrap resampling method has been applied to calculate the outcomes presented in Table I as well. In particular, the

TABLE I. Results of ν and g_c obtained from the Bayesian analysis and bootstrap resampling procedures.

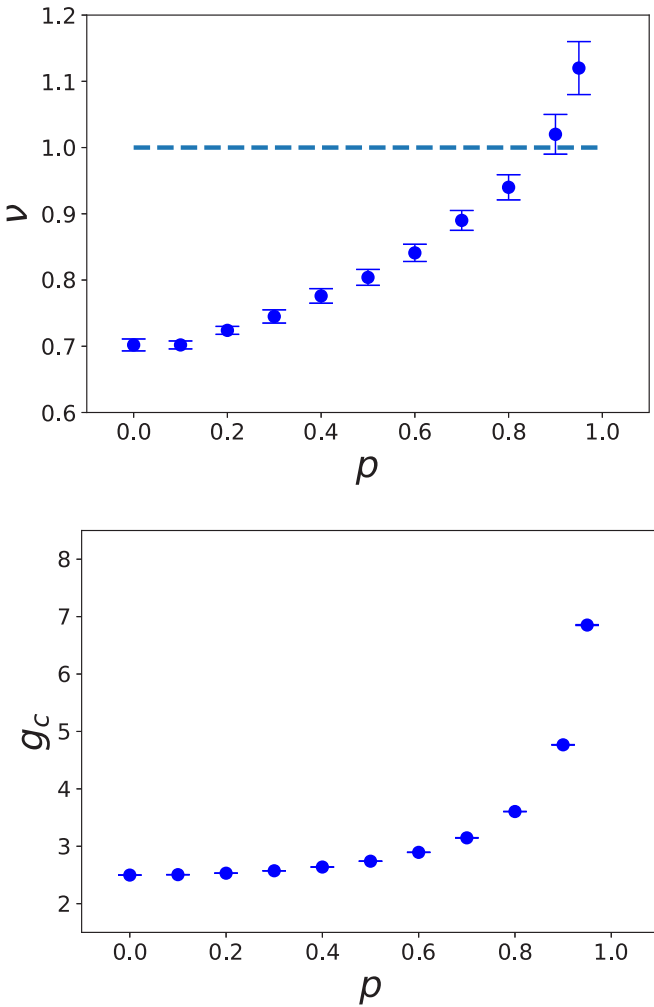| p	ν	g_c
0.0	0.702(9)	2.4981(2)
0.1	0.702(6)	2.5056(2)
0.2	0.724(6)	2.5308(4)
0.3	0.745(10)	2.5732(7)
0.4	0.776(11)	2.6383(11)
0.5	0.804(12)	2.7397(13)
0.6	0.841(13)	2.8939(20)
0.7	0.890(15)	3.1466(38)
0.8	0.940(19)	3.605(15)
0.9	1.02(3)	4.767(40)
0.95	1.12(4)	6.853(77)

FIG. 4. ν (top) and g_c (bottom) as functions of p. The horizontal dashed line in the top panel represents the threshold for which the Harris criterion is fulfilled for the considered models.

means and errors shown in the table are related to the means and standard deviations of the distributions resulting from the weighted bootstrap resampling procedures. The details of the Bayesian analysis, as well as the resampling procedures are outlined in the Appendix.

ν and g_c as functions of p are presented in Fig. 4 for visualizing the trend of these two obtained quantities with respect to p. In particular, the horizontal dashed line shown in the top panel of Fig. 4 represents the threshold for which the Harris criterion is fulfilled for the considered models.

For the clean model, the averaged g_c and ν are given by 2.4981(2) and 0.702(9), respectively. The calculated g_c is in nice agreement with the known results in the literature [42]. The determined ν for $p = 0$ is slightly smaller in magnitude than the expected $O(3)$ value 0.7112(5). The largest L used in the simulations conducted here is $L = 48$. As a result, the small deviation between 0.702(9) found here and 0.7112(5) can be easily accounted for by the cubic term introduced in Ref. [42] which will lead to anomalous large finite-size correction.

Table I also implies that g_c grows with p. The most remarkable outcome shown in Table I is that, as the magnitude

of p rises, the corresponding ν calculated increases in size gradually from that of $p = 0$ as well. Particularly for $p \geqslant 0.3$ and $p \leqslant 0.8$, the obtained ν's from Bayesian analysis are all statistically larger than 0.7112(5), but smaller than 1.0. In addition, for $p = 0.9$ and $p = 0.95$, the associated ν's are around 1.0 with which the Harris criterion $\nu \geqslant 2/d$ is satisfied. Here we would like to point out that in Table I, the quoted errors can be interpreted as generalized standard deviations. The standard deviations directly calculated from the associated distributions are the errors of means and have much smaller magnitude than those shown in Table I. As a result, it is beyond doubt that the ν of $p = 0.9$ and $p = 0.95$ fulfill the Harris criterion.

To summarize, the outcomes of our investigation, as shown in Table I, indicate that for each employed p such that $0.3 \leqslant p \leqslant 0.8$, the resulting associated correlation length exponent neither stays as the $O(3)$ value $\nu = 0.7112(5)$ nor satisfies the Harris criterion $\nu \geqslant 2/d = 1$. Moreover, for $p \geqslant 0.9$, the Harris criterion is fulfilled. The results concluded here implies it is highly plausible that there exists a p_c so that the ν, which corresponds to p greater (smaller) than p_c, will fulfill (violate) the Harris criterion. From the considered quantum spin system, we arrive at a scenario regarding the connection between ν and quenched disorder with a tunable randomness strength.

It should be pointed out that the ν determined from Q_1 differs from that related to Q_2 slightly. We attribute this to corrections not taken into account in the analysis. Despite this, it is without doubt that both Q_1 and Q_2 will lead to the scenario described above.

Based on the explicit expression of the disorder taken into account here, one expects that the obtained scenario should still be valid for other randomness distributions using a similar idea as the one investigated above. Motivated by this intuitive thought, apart from simulating the disordered system introduced previously, we have considered a quenched disorder for the plaquette model (the right-hand panel of Fig. 1). Specifically, each of the bold bonds takes the antiferromagnetic strength of $(1 + K)J_c$ and $(1 - K)J_c$ with probability P and $1 - P$, respectively. Here $0 < P < 1$ and we have used $K = 0.5$. In addition, the J_c appearing above is given by 1.8230 which is the critical point of the clean plaquette model. With such a setup, P is the tunable variable for this model.

The resulting Q_1 and Q_2 of this model with this type of quenched disorder are shown in Fig. 5. Moreover, by applying typical fits with the conventional finite-size scaling equations to Q_1 and Q_2, we arrive at $\nu = 0.79(2)$ [and the critical point $P_c = 0.5520(16)$]. This number $\nu = 0.79(2)$ is without doubt statistically different from both 0.7112(5) and 1. By changing K continuously, it is anticipated that the corresponding ν will vary in a gradual manner. This is of high similarity to the scenario associated with the herringbone model found earlier in this study.

IV. DISCUSSION AND CONCLUSIONS

According to Ref. [43], based on the procedure of scaling employed in this study, the Harris criterion should be $\nu_{\text{FS}} \geqslant 2/d$, where the subscript FS stands for finite size. In particular, Ref. [43] also demonstrates that the bulk correlation length
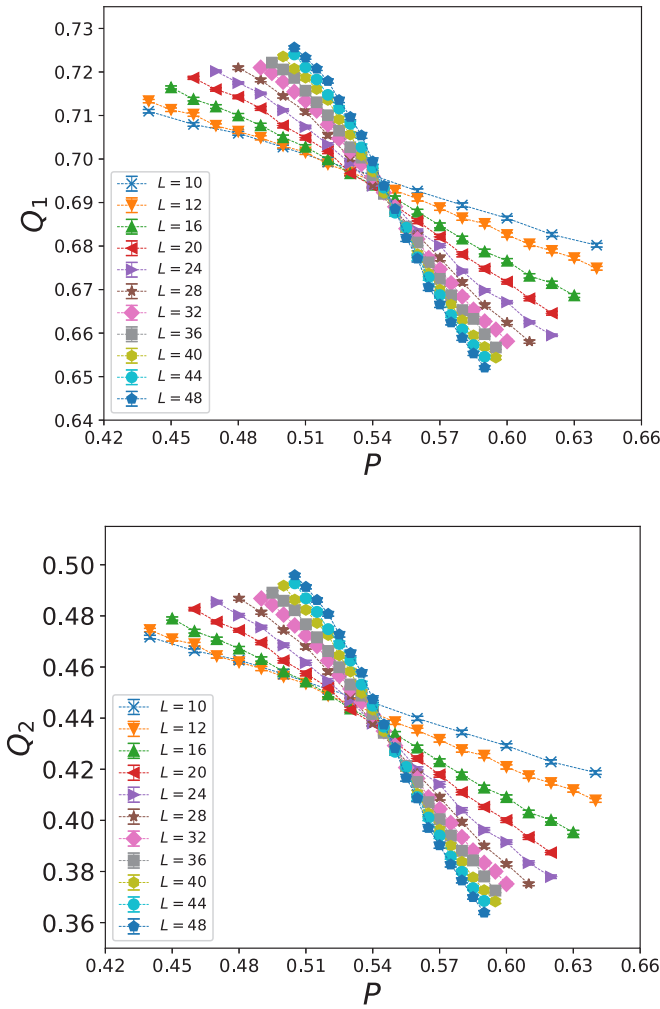
FIG. 5. Q_1 (top) and Q_2 (bottom) as functions of P for the considered disordered plaquette model studied here. Dashed lines are added to guide the eye.

ν can be obtained by a modified procedure and may violate the Harris criterion. Considering the facts that most of the outcomes obtained in this study violate $\nu_{FS} \geqslant 2/d$ and the variation among all the $g_c(p)$ determined here is not small, the observed scenario cannot be easily accounted for by the arguments in Ref. [43]. Results of some studies such as Refs. [10,44] imply that the values of ν (or ν_{FS}) calculated do not depend on the disorder strength. The scenario found in this study clearly is different from this and other established ones in the literature [10,44,45].

We would like to re-emphasize the following points. First of all, the ν_{FS} obtained here for $p \geqslant 0.3$ all violate the Harris criterion $\nu_{FS} \geqslant 2/d$ except for $p = 0.9$ and 0.95. Second, for any given p, the phase transition is due to dimerization, namely two nearest-neighboring spins (on the lattice) form a singlet. Hence, theoretically it is anticipated that for two close-by values of p, say $p = 0.3$ and $p = 0.4$, the calculated results of ν should be close to each other or even consistent within statistical error. As can be seen from Table I, this is not the case. In particular, the difference of the g_c between $p = 0.0$ and $p = 0.3$ is only around 3%, yet a new critical exponent ν emerges for $p = 0.3$. It is interesting as well to notice that

while in [10] the g_c of the configurational random plaquette model varies from that of its clean counterpart by 4%, both models have the same $O(3)$ exponent $\nu = 0.7112(5)$. Therefore, the closeness of the critical point of a disordered system to that of its clean analog, which may be interpreted as the statement "remains well defined" in the Harris criterion, is not crucial for the appearance of a new universality class.

Interestingly, based on the outcomes found here, it is likely that for the considered model with the designed quenched disorder, the largest value of ν one can obtain should be around 1.1–1.2. This number agrees with the results calculated by simulating quantum spin models on the bilayer lattice with site and bond dilution [19,20]. It is plausible that for a disordered spin-1/2 system, whenever the associated ν fulfills the Harris criterion, its value is in the range of 1–1.2. Finally, it will be intriguing as well to examine whether there is a connection between the scenario found here and the long crossover observed in Ref. [46].

In conclusion, in order to obtain a theoretical explanation for the exotic scenario observed in this study, a detailed exploration of the relevant theory other than what has been accomplished for the Harris criterion is required.

APPENDIX: DETAILS OF THE BAYESIAN ANALYSIS

In this Appendix, we brief describe how the outcomes shown in the main text are obtained from the relevant data. The method used in obtaining the corresponding results of ν and g_c from the data of Q_1 and Q_2 is the Bayesian analysis. The models considered for the Bayesian analysis are the expected finite-size scaling *Ansätze* for Q_1 and Q_2:

$$y = (1 + a_0 L^{-\omega})[a_1 + a_2(tL^{1/\nu}) + a_3(tL^{1/\nu})^2 + a_4(tL^{1/\nu})^3 + \cdots], \tag{A1}$$

where a_i for $i = 0, 1, 2, 3, \ldots$ are some constants. Moreover, in Bayesian frameworks the posterior probability distribution is used to evaluate the statistical uncertainties of parameters in Eq. (A1). For a given data set $(\mathbf{x}, \mathbf{y})$ and a model, let $\theta = (a_0, a_1, a_2, a_3, \ldots)$, then the posterior in Bayesian statistics is the conditional probability function of the model's parameters and has the following expression:

$$P(\theta|\mathbf{x}) = \frac{L(\mathbf{x}|\theta)\pi(\theta)}{M(\mathbf{x})}, \tag{A2}$$

where $\mathbf{x}$ is assumed to be sampled from the distribution of $\mathbf{X}(\theta)$, $L(\mathbf{x}|\theta)$ is the likelihood, $\pi(\theta)$ is the prior, and $M(\mathbf{x})$ is the evidence. In this study $\mathbf{X}(\theta)$ is assumed to be independent Gaussian distributions, whose mean and standard deviation are $y_i(\theta)$ and σ_i. Therefore, the likelihood can be written as

$$L(\mathbf{x}|\theta) = \prod_i \frac{1}{\sqrt{2\pi}\sigma_i} \exp\left[-\left(\frac{y_i(\theta) - x_i}{\sigma_i}\right)^2\right]. \tag{A3}$$

TABLE II. Results of g_c and ν for $p = 0.5$. The outcomes shown in the second (third) and fourth (fifth) columns are calculated using the conventional fits and Bayesian analysis, respectively. The numbers associated with L_m and $tL^{1/\nu}$ appearing in the first column are the minimum box size and the order of polynomials in $tL^{1/\nu}$ (including subleading correction) considered in the analysis.

$(Q_i, L_m, tL^{1/\nu})$	g_c	ν	g_c	ν
$(Q_1, 8, 3)$	2.7381(11)	0.813(5)	2.7378(11)	0.812(4)
$(Q_1, 8, 4)$	2.7385(11)	0.813(5)	2.7384(11)	0.812(4)
$(Q_1, 8, 5)$	2.7395(13)	0.806(5)	2.7392(12)	0.805(4)
$(Q_1, 12, 3)$	2.7379(12)	0.807(5)	2.7377(11)	0.807(5)
$(Q_1, 12, 4)$	2.7383(13)	0.807(5)	2.7383(12)	0.805(5)
$(Q_1, 12, 5)$	2.7392(14)	0.803(5)	2.7388(14)	0.803(5)
$(Q_1, 16, 3)$	2.7382(12)	0.805(6)	2.7378(10)	0.805(5)
$(Q_1, 16, 4)$	2.7384(12)	0.804(6)	2.7381(10)	0.804(5)
$(Q_1, 16, 5)$	2.7390(13)	0.804(6)	2.7385(11)	0.804(5)
$(Q_2, 8, 3)$	2.7393(12)	0.796(5)	2.7391(11)	0.794(4)
$(Q_2, 8, 4)$	2.7398(12)	0.795(5)	2.7396(11)	0.795(4)
$(Q_2, 8, 5)$	2.7402(13)	0.791(5)	2.7404(12)	0.792(4)
$(Q_2, 12, 3)$	2.7392(13)	0.792(5)	2.7388(12)	0.793(5)
$(Q_2, 12, 4)$	2.7398(13)	0.792(5)	2.7397(13)	0.793(5)
$(Q_2, 12, 5)$	2.7405(15)	0.790(5)	2.7405(14)	0.790(5)
$(Q_2, 16, 3)$	2.7395(12)	0.792(6)	2.7390(10)	0.792(5)
$(Q_2, 16, 4)$	2.7399(12)	0.792(6)	2.7394(11)	0.792(5)
$(Q_2, 16, 5)$	2.7404(15)	0.793(5)	2.7398(12)	0.793(5)

The Bayesian frameworks requires certain prior to begin with and here we consider flat prior in a certain range, namely $-10 < a_0 < 10$, $0 < \omega < 5$, $0.5 < \nu < 1.5$, and zero otherwise, where a_0 is the coefficient in front of the term $L^{-\omega}$.

TABLE III. Results of g_c and ν for $p = 0.9$. The outcomes shown in the second (third) and fourth (fifth) columns are calculated using the conventional fits and Bayesian analysis, respectively. The numbers associated with L_m and $tL^{1/\nu}$ appearing in the first column are the minimum box size and the order of polynomials in $tL^{1/\nu}$ (including subleading correction) considered in the analysis.

| $(Q_i, L_m, tL^{1/\nu})$	g_c	ν	g_c	ν
$(Q_1, 8, 3)$	4.815(9)	1.080(9)	4.826(18)	1.084(10)
$(Q_1, 8, 4)$	4.816(10)	1.084(9)	4.827(14)	1.089(10)
$(Q_1, 8, 5)$	4.815(10)	1.081(9)	4.831(14)	1.086(10)
$(Q_1, 12, 3)$	4.807(12)	1.051(10)	4.812(13)	1.052(10)
$(Q_1, 12, 4)$	4.810(12)	1.053(9)	4.816(15)	1.051(10)
$(Q_1, 12, 5)$	4.810(12)	1.052(9)	4.814(15)	1.052(10)
$(Q_1, 16, 3)$	4.798(13)	1.037(10)	4.807(15)	1.040(10)
$(Q_1, 16, 4)$	4.803(14)	1.035(10)	4.821(16)	1.038(10)
$(Q_1, 16, 5)$	4.801(14)	1.034(10)	4.820(16)	1.039(10)
$(Q_2, 8, 3)$	4.817(13)	1.044(8)	4.817(13)	1.045(8)
$(Q_2, 8, 4)$	4.812(14)	1.045(8)	4.812(13)	1.044(8)
$(Q_2, 8, 5)$	4.813(14)	1.045(8)	4.814(13)	1.044(8)
$(Q_2, 12, 3)$	4.828(15)	1.030(9)	4.833(17)	1.031(9)
$(Q_2, 12, 4)$	4.825(17)	1.029(9)	4.829(17)	1.030(9)
$(Q_2, 12, 5)$	4.826(17)	1.029(9)	4.831(18)	1.030(9)
$(Q_2, 16, 3)$	4.820(14)	1.021(9)	4.839(18)	1.023(10)
$(Q_2, 16, 4)$	4.821(14)	1.017(9)	4.842(18)	1.022(10)
$(Q_2, 16, 5)$	4.818(15)	1.017(9)	4.838(19)	1.023(10)
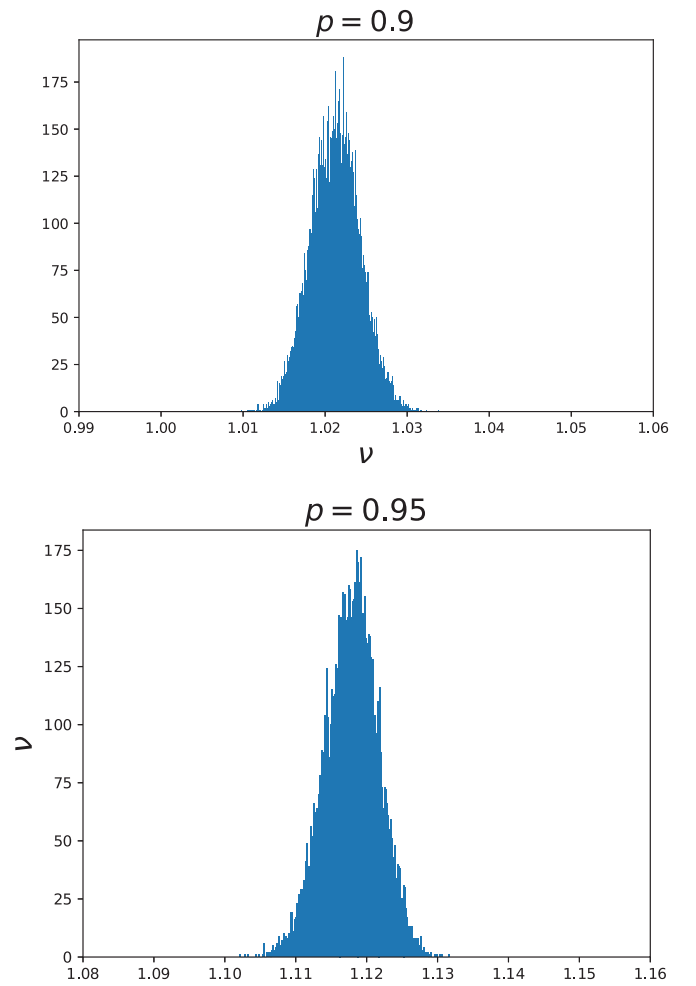
FIG. 6. Distributions of ν for $p = 0.9$ (top) and $p = 0.95$ (bottom) obtained from the weighted bootstrap resampling procedure.

By taking into account the fact that b and ω are the subleading corrections to scaling, it is legitimate to put such constraints on b and ω. To make sure that the prior chosen would not affect the results of g_c and ν, we have shifted the range of the prior to be narrower ($-5 < a_0 < 5$ and $0 < \omega < 3$), and have seen no significant changes of g_c and ν from the statistics perspective. Finally, since $M(\mathbf{x})$ in Eq. (A2) is not a function of θ, it can be ignored.

It should be pointed out that it is not easy to construct the distribution of the posterior due to lots of dimension in the parameter space. Conventionally, Markov chain Monte Carlo (MCMC), which is a sampling technique in continuous parameter space, can solve this problem efficiently. Details of the full Bayesian analysis procedure and the relevant codes used here can be found in Refs. [41,47].

The outcomes of ν and g_c determined from the Bayesian analysis are the *maximum a posterior* estimations (which is defined as the result of having the least value of χ^2/DOF in this study due to the flat prior used here). In addition, the associated uncertainties are the standard deviations of the posterior distributions. For each p and a fixed L_m (L_m is the smallest box size used in the analysis), several examinations with various range of g are performed using the Bayesian method. When estimating the means and uncertainties of g_c
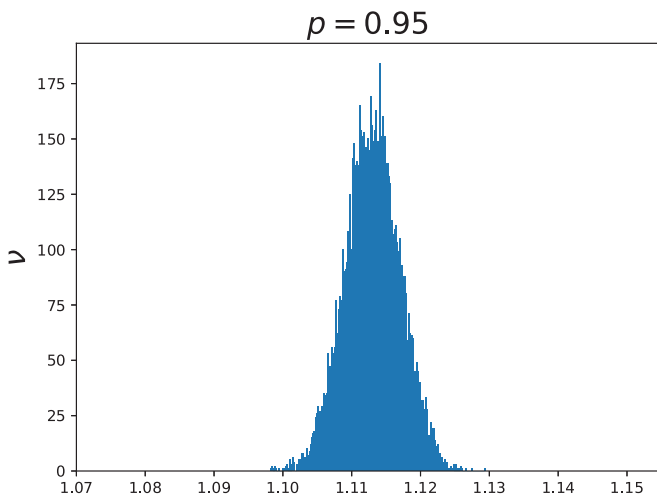
FIG. 7. Distribution of ν for $p = 0.95$. The result is calculated using the standard bootstrap resampling method.
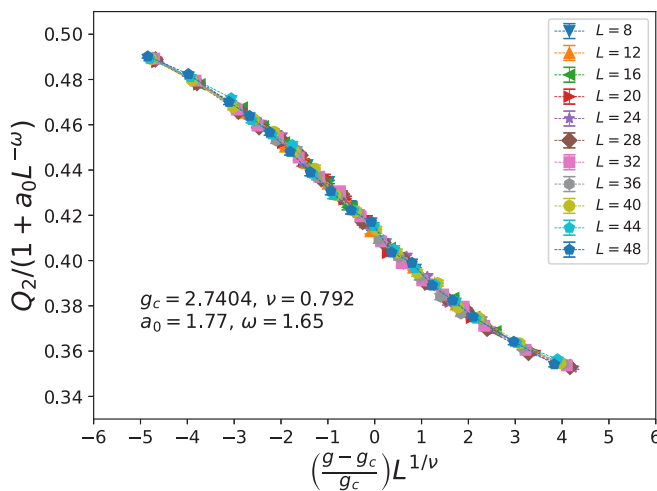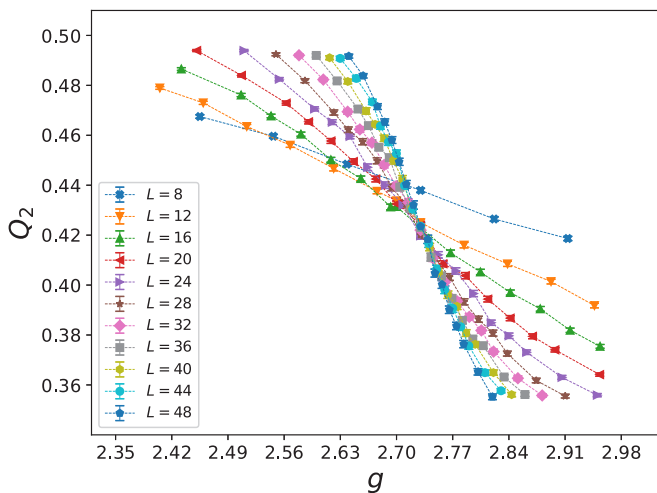

FIG. 8. Q_2 (top) of $p = 0.5$ and the corresponding data collapse (bottom) for the considered disordered herringbone model studied here. Dashed lines are added to guide the eye. The g_c, ν, a_0, and ω shown in the bottom figure, which are used to produce the demonstrated results, are obtained from one of the many associated analyses.
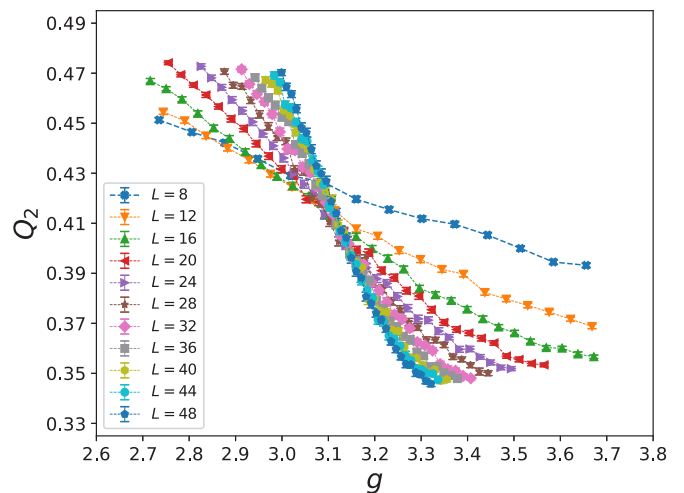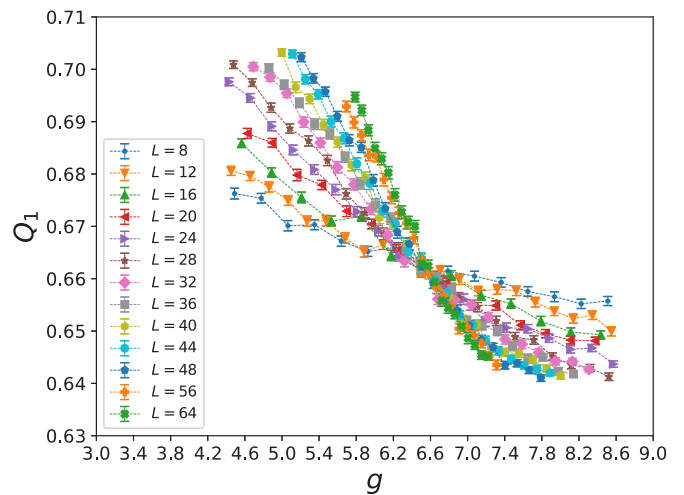

FIG. 9. Q_1 (top, $p = 0.95$) and Q_2 (bottom, $p = 0.7$) as functions of g for the considered disordered herringbone model studied here. Dashed lines are added to guide the eye.

and ν for a given p, one has to pay attention to the fact that results determined using various conditions such as L_m and the order of the finite-size scaling ansatz are correlated.

Tables II and III list the comparison between the results obtained by the conventional fits and the Bayesian analysis for $p = 0.5$ and $p = 0.9$. In addition, most available data are considered when carrying out the calculations. The consistency shown in these two tables suggests that the the outcomes determined by the Bayesian analysis are reliable.

Empirically, one can check the convergence of the obtained results by eliminating data of small L gradually. Indeed, for large p the ν we calculate has a trend of becoming smaller as one deletes more and more small L data in the analysis. While such a strategy is adopted in most numerical studies, it does not seem to be based on any rigorous arguments. Particularly, with such a procedure, results are more and more correlated since fewer and fewer data are considered in the analysis. In addition, disregarding the outcomes which have good χ^2/degree of freedom and are obtained by considering data containing those of small L may lead to biased conclusions. To avoid biased results arising from

using only data of larger L as well as other factors that may lead to systematic uncertainties, we employ the following procedures when analyzing the data. Specifically, to calculate the means and errors of the desired quantities appropriately, for each considered p the weighted bootstrap resampling method is applied to all the results associated with it. In other words, for every randomly generated data set $\{(g_{c,i}, \sigma_{g_{c,i}})\}$ obtained using the bootstrap procedure ($\sigma_{g_{c,j}}$ is the standard deviation associated with $g_{c,j}$), the resulting mean is given by

$$\frac{\sum_i \frac{1}{\sigma_{g_{c,i}}^2} g_{c,i}}{\sum_i \frac{1}{\sigma_{g_{c,i}}^2}}. \tag{A4}$$

Such an idea of using weighted mean is based on the fact that data with large standard deviations are less accurately determined than those with small standard deviations. Hence when carrying out every bootstrap resampling step, the data that come with large standard deviations should take less weight in calculating the associated mean. A similar procedure applies to the determination of ν as well.

After carrying out the ten (or twenty) thousand bootstrap resampling steps described above, the final outcomes of g_c and ν for each of the employed p, which are presented in Table 1 of the main text, are the mean and the standard deviation times $\sqrt{N_p}$ of the obtained distribution [48]. Here N_p is the number of data points (associated with p) used in the resampling procedure. The standard deviations calculated directly from the distributions are the errors for means, and have much smaller magnitude than those calculated using the one defined above.

Figure 6 shows the resulting distributions of ν for 0.9 and 0.95 (top and bottom panels, respectively) obtained from the weighted bootstrap resampling procedure. Based on the results demonstrated in that figure, there are very high probabilities that the ν associated with $p = 0.9$ and 0.95 satisfy the Harris criterion.

We have also performed the standard bootstrap resampling procedure and have arrived at the same conclusions as those associated with the weighted one; see Fig. 7.

Finally, it should be pointed out that for large p, especially for $p = 0.9$ and 0.95, the calculated g_c and ν do slightly depend on several factors such as the range of g and L considered in the analysis. For instance, the magnitude of ν is diminished a bit when data of small L are excluded in the analysis. In spite of this, it is beyond doubt that the ν's corresponding to $p \geqslant 0.9$ fulfill the Harris criterion.

For convenience, some data of $p = 0.5$, $p = 0.7$, and $p = 0.95$ are presented in Figs. 8 and 9.

[1] D. S. Fisher, Phys. Rev. B **50**, 3799 (1994).

[2] O. Vajk, P. Mang, M. Greven, P. Gehring, and J. Lynn, Science **295**, 1691 (2002).

[3] A. W. Sandvik, Phys. Rev. B **66**, 024418 (2002).

[4] G. A. Csáthy, J. D. Reppy, and M. H. W. Chan, Phys. Rev. Lett. **91**, 235301 (2003).

[5] Y.-C. Lin, R. Mélin, H. Rieger, and F. Iglói, Phys. Rev. B **68**, 024424 (2003).

[6] Y.-C. Lin, H. Rieger, N. Laflorencie, and F. Iglói, Phys. Rev. B **74**, 024427 (2006).

[7] N. Laflorencie, S. Wessel, A. Läuchli, and H. Rieger, Phys. Rev. B **73**, 060403(R) (2006).

[8] T. Vojta, J. Phys. A **39**, R143-R205 (2006).

[9] T. Vojta, J. Low Temp. Phys. **161**, 299 (2010).

[10] D.-X. Yao, J. Gustafsson, E. W. Carlson, and Anders W. Sandvik, Phys. Rev. B **82**, 172409 (2010).

[11] P. Carretta, G. Prando, S. Sanna, R. De Renzi, C. Decorse, and P. Berthet, Phys. Rev. B **83**, 180411(R) (2011).

[12] R. Yu, C. F. Miclea, F. Weickert, R. Movshovich, A. Paduan-Filho, V. S. Zapf, and T. Roscilde, Phys. Rev. B **86**, 134421 (2012).

[13] R. Yu, L. Yin, N. S. Sullivan, J. S. Xia, C. Huan, A. Paduan-Filho, N. F. Oliveira, Jr., S. Haas, A. Steppke, C. F. Miclea, F. Weickert, R. Movshovich, E.-D. Mun, B. L. Scott, V. S. Zapf, T. Roscilde, and A. Kitaev, Nature (London) **489**, 379 (2012).

[14] T. Vojta, in *Lectures on the Physics of Strongly Correlated Systems XVII: Seventeenth Training Course in the Physics of Strongly Correlated Systems*, edited by A. Avella and F. Mancini, AIP Conf. Proc. No. 1550 (AIP, Melville, NY, 2013), p. 188.

[15] N. Ma, A. W. Sandvik, and D.-X. Yao, Phys. Rev. B **90**, 104425 (2014).

[16] A. B. Harris, J. Phys. C **7**, 1671 (1974).

[17] J. T. Chayes, L. Chayes, D. S. Fisher, and T. Spencer, Phys. Rev. Lett. **57**, 2999 (1986).

[18] O. Motrunich, S. C. Mau, D. A. Huse, and D. S. Fisher, Phys. Rev. B **61**, 1160 (2000).

[19] A. W. Sandvik, Phys. Rev. Lett. **89**, 177201 (2002).

[20] O. P. Vajk and M. Greven, Phys. Rev. Lett. **89**, 177202 (2002).

[21] R. Sknepnek, T. Vojta, and M. Vojta, Phys. Rev. Lett. **93**, 097201 (2004).

[22] R. Yu, T. Roscilde, and S. Haas, Phys. Rev. Lett. **94**, 197204 (2005)

[23] A. W. Sandvik, Phys. Rev. Lett. **96**, 207201 (2006).

[24] J. A. Hoyos *et al.*, Europhys. Lett. **93**, 30004 (2011).

[25] T. Vojta and J. A. Hoyos, Phys. Rev. Lett. **112**, 075702 (2014).

[26] M. Schrauth, J. S. E. Portela, and F. Goth, Phys. Rev. Lett. **121**, 100601 (2018).

[27] T. Vojta, Annu. Rev. Condens. Matter Phys. **10**, 233 (2019).

[28] N. Goldenfeld, *Lectures on Phase Transitions and the Renormalization Group*, Frontiers in Physics (CRC Press, Boca Raton, FL, 1992).

[29] M. Campostrini, M. Hasenbusch, A. Pelissetto, P. Rossi, and E. Vicari, Phys. Rev. B **65**, 144520 (2002).

[30] A. Pelissetto and E. Vicari, Phys. Rep. **368**, 549 (2002).

[31] L. Wang, K. S. D. Beach, and A. W. Sandvik, Phys. Rev. B **73**, 014431 (2006).

[32] A. F. Albuquerque, M. Troyer, and J. Oitmaa, Phys. Rev. B **78**, 132402 (2008).

[33] S. Wenzel and W. Janke, Phys. Rev. B **79**, 014410 (2009).

[34] L. D. Carr, *Understanding Quantum Phase Transitions*, Condensed Matter Physics (CRC press, Boca Raton, FL, 2010).

[35] S. Sachdev, *Quantum Phase Transitions*, 2nd ed. (Cambridge University Press, Cambridge, UK, 2011).

[36] K. Binder, Z. Phys. B **43**, 119 (1981).

[37] A. W. Sandvik, Phys. Rev. B **59**, R14157(R) (1999).

[38] A. W. Sandvik, in *Lectures on the Physics of Strongly Correlated Systems XIV: Fourteenth Training Course in the Physics of Strongly Correlated Systems*, edited by A. Avella and F. Mancini AIP Conf. Proc. No. 1297 (AIP, New York, 2010), p. 135.

[39] K. Harada, Phys. Rev. E **84**, 056704 (2011).

[40] K. Harada, Phys. Rev. E **92**, 012106 (2015).

[41] D. Foreman-Mackey, D. W. Hogg, D. Lang, and J. Goodman, Pub. Astron. Society Pacific **125**, 306 (2013).

[42] L. Fritz, R. L. Doretto, S. Wessel, S. Wenzel, S. Burdin, and M. Vojta, Phys. Rev. B **83**, 174416 (2011).

[43] F. Pázmándi, R. T. Scalettar, and G. T. Zimányi, Phys. Rev. Lett. **79**, 5130 (1997).

[44] J. Kisker and H. Rieger, Phys. Rev. B **55**, R11981 (1997).

[45] F. Pázmándi and G. T. Zimányi, Phys. Rev. B **57**, 5044 (1998).

[46] J. C. Getelina, F. C. Alcaraz, and J. A. Hoyos, Phys. Rev. B **93**, 045136 (2016).

[47] https://emcee.readthedocs.io/en/stable/.

[48] The results presented in Table I of the main text are slightly different from those shown in a previous version of this paper (however, they are statistically consistent). This is because an alternative analysis method was used there.